ACS Sustainable Chemistry & Engineering

pubs.acs.org/journal/ascecg

Research Article

Effects on the Physicochemical Properties of Hydrochar Originating from Deep Eutectic Solvent (Urea and $ZnCl_2$)-Assisted Hydrothermal Carbonization of Sewage Sludge

Zhixiang Xu,* Xueqin Ma, Junjie Liao, Sameh M. Osman, Shiyong Wu,* and Rafael Luque*

Cite This: *ACS Sustainable Chem. Eng.* 2022, 10, 4258−4268

Read Online

ACCESS | Metrics & More | Article Recommendations | Supporting Information

ABSTRACT: Deep eutectic solvents (DESs) ($ZnCl_2$ and urea) have been used to solubilize organic matter from sewage sludge (SS), followed by subsequent hydrothermal carbonization (HTC) to obtain low-nitrogen-content hydrochar. The nitrogen content in hydrochar obtained after DES addition decreased to 1.93 from 3.15% (no DES) at 210 °C. DES can notably dissolve proteins and lipids during HTC of SS. HTC of polysaccharides was enhanced, increasing the degree of carbonization. The key role of DES in SS during HTC was the dissolution of proteins, promoting carbonization of polysaccharides, Maillard reactions, deamination, and decarboxylation of proteins. $ZnCl_2$ was probably converted into β-Zn(OH)C1 and ZnO during HTC. Results pointed to relevant enhancements when DES was added, useful for organic waste valorization such as SS, food waste, poultry manure, and related waste feedstock.

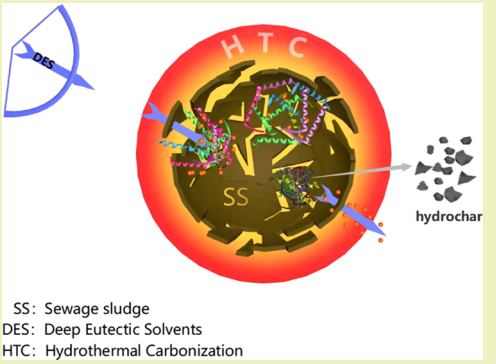

KEYWORDS: *sewage sludge, deep eutectic solvents, hydrothermal carbonization, catalysis*

INTRODUCTION

Activated sewage sludge (SS), a byproduct of wastewater treatment, attracts attention worldwide due to inherent challenges and environmental impacts related to its difficult management. Significantly, the disruption of extracellular polymeric substances (EPSs) is difficult since it can influence the dewatering and utilization of organic matter.[1,2] Hydrothermal carbonization (HTC) has received significant attention due to needing mild reaction conditions that avoid feedstock drying and obtaining solid as a fuel.[3] The HTC of SS, which contains proteins, polysaccharides, lipids, and other organic matter,[4] has been the subject of extensive investigations, including solid fuel, N-carbon, catalysis HTC, etc.[3,5−9]

EPS and cell walls of SS are challenging to disrupt because of the strong hydrogen bonding, resulting in a low degree of carbonization, high nitrogen content, and partial unconverted feedstock present in hydrochar.[6] The stability of the EPS structure makes the treatment of SS challenging, including dewatering,[10] HTC,[9] pyrolysis,[11] and so on. Therefore, disrupting the floc structure of SS to utilize organic matter effectively has become a very important issue. A low degree of carbonization in SS would indicate a high nitrogen content in hydrochar since the main organic matter is the protein in SS.[3] Possibly, the main reason for the low degree of carbonization is that the organic matter in SS has a huge molecular weight and a strong hydrogen bond between different biopolymers, resulting in limited hydrolysis under HTC conditions.[12]

In our previous work,[6] hydrotalcites were used to disrupt the floc structure of SS in order to release the organic matter, which in turn can decrease the nitrogen content in hydrochars. Conventional methods including acidic and alkaline catalyses and thermal hydrolysis are limited in the disruption of the floc structure of SS.[13] Recently, ultrasonic pretreatment was used to disrupt the EPS and cell wall to promote organic matter release from SS.[14] Hydrolysis, dehydration, and decarboxylation were enhanced during HTC after ultrasonic pretreatment. On the other hand, advanced oxidation processes (AOPs, like H_2O_2 and persulfate) have been widely used to destroy the floc structure to promote SS dewatering.[15] Recently, AOP coupled with thermal treatment was also developed.[16] This method was mainly carried out below 100 °C, resulting in the limited disruption of the floc structure of SS. Recently, Ning et al. have reported using persulfate as an oxidant to destroy the EPS structure and carry out HTC.[17] The result showed that the Fe(II)-activated persulfate system could destroy the EPS structure of SS and facilitate nitrogen element removal in hydrochar. Wang et al. reported the use of H_2O_2 as an oxidant and fly ash as the skeleton material to further remove nitrogen

Received: January 5, 2022
Revised: March 11, 2022
Published: March 23, 2022

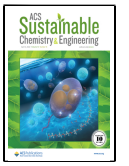

https://doi.org/10.1021/acssuschemeng.2c00086
ACS Sustainable Chem. Eng. 2022, 10, 4258−4268

and sulfur contents in hydrochar during HTC of SS.[18] However, the disruption of EPS was still limited because of the limited amount of oxidant that was quickly depleted. Hence, developing a new method to destroy the EPS structure of SS is very important.

Deep eutectic solvents (DESs) have been considered as green solvents with specific and unique physicochemical properties, which can be utilized in different fields. DESs have received increasing attention in the past two decades.[19−22] DESs could be prepared by a two- or three-component combination with a specific ratio of hydrogen-bond acceptors and hydrogen-bond donors to change the properties of the target compound.[23] In biomass treatment, DESs can selectively solubilize large amounts of lignin but not cellulose, which can be further utilized to produce biogas; however, it is still a pretreatment technology.[24,25] On the other hand, DESs can also help prepare a new type of carbonaceous material to be utilized in the electrochemistry field.[26−28] Above all, DES is a promising green solvent in terms of organic matter separation, especially in biomass application.

To obtain a low nitrogen content of hydrochar, the EPS structure of SS should be first disrupted. DES has been introduced during HTC using DES as a solvent and catalyst to effectively disrupt the EPS structure. Additionally, Cl^- has been demonstrated to have a positive effect on the HTC of SS.[8,14] Hence, in this contribution, DES ($ZnCl_2$ + urea) was added to investigate its influence on this process, especially decreasing the nitrogen content in the prepared hydrochars. SS was also soaked in the DES solution with a set time to explore the dissolution role of DES on the HTC of SS. Both aqueous phase and hydrochar properties were investigated. Importantly, $ZnCl_2$ has also been widely used as an activation agent for the preparation of activated porous carbons, while urea is crucial to introduce nitrogen-containing surface functionalities even to graphitic carbon nitride clusters/phases. The obtained results would provide a better understanding of the HTC process.

MATERIALS AND METHODS

Materials. SS was supplied by the Gujing group wastewater treatment plant located in Bozhou, Anhui Province, China. The moisture and ash content (dry matter) of SS were 85.2 and 38.7%, respectively. $ZnCl_2$ and urea were of analytical grade and were not further purified.

HTC Experiments. Typically, the molar ratio of $ZnCl_2$/urea was 1:3.5. A total of 15 g of SS and 15 g of H_2O were directly poured into a reactor to carry out a blank experiment. DES was loaded at mass ratios of 5 and 10% to the SS, separately. Then, the mixture was poured into the reactor to carry out the HTC experiment. On the other hand, SS was soaked in the DES solution for 2 and 5 h, in which the mole ratio of $ZnCl_2$/urea was still 1:3.5. Then, the mixture was directly poured into the reactor to carry out HTC experiments. HTC experiments were carried out in a stainless-steel reactor (50 mL in volume, GSHA-0.5, China). In each experiment, the reactor was sealed, heated to the desired temperature, and held at the desired temperature for 60 min without a mixer. When the temperature reached the setting value, the time was recorded. When the reaction time was reached, the reactor was stopped being heated and cooled down to room temperature. Solid and aqueous phase mixtures were separated using vacuum filtration. The solid phase was heated to 105 °C for 24 h before further analysis, and then, it was analyzed by elemental analysis and Fourier transform infrared spectroscopy (FTIR). The aqueous phase was collected for further analysis for total organic carbon (TOC), total nitrogen (TN), and NH_3-N. Each experiment was repeated three times.

Analytical Methods. A TOC analyzer (Shimadzu TOC-VCSH, Japan) was used to detect the TOC value of the aqueous phase. TN was measured using the standard method (HJ 636−2012 China). NH_3-N was measured using the spectrophotometry method based on the Chinese standard method (HJ 535−2009 China). The three-dimensional-excitation-emission-matrix (3D-EEM) fluorescence spectra of the aqueous phase were measured with a Hitachi Fluorescence Spectrophotometer-F7000 at room temperature. Fluorescence region integration was performed to obtain the total fluorescence intensity of these substances under different experimental conditions. The detailed information can be found in our previous work.[29]

The elemental compositions of hydrochar samples were measured by an elemental analyzer (Flash 2000 CHNS/O, Thermo Fisher Scientific) with the combustion method. According to elemental analysis results, the higher heating values (HHVs) of hydrochars were calculated using the Dulong formula (heating value (MJ/kg) = 0.338 C + 1.428 (H-O/8) + 0.095 S),[30] where C, H, O, and S are the wt % of each individual element. X-ray diffraction (XRD) analysis of the hydrochar samples was performed over the Bruker D8 with α-radiation by Cu Kα at room temperature. The scanning rate was 6°/min in the range of 5−90°. Thermal decomposition properties of hydrochar samples were analyzed by a thermogravimetry (TG) analyzer (NETZSCH5, Germany). The condition was that about 10 mg of hydrochar sample was carried out in a ceramic crucible under a N_2 atmosphere as the carrier gas at a 50 mL/min flow rate and heated from room temperature to 900 °C at the heating rate of 20 °C/min. The morphology was probed to determine the surface characteristics of hydrochar from a scanning electron microscope (SEM, Merlin, Zeiss). FTIR of the hydrochar was performed by a Nicolet iS50 FTIR spectrometer (Thermo Scientific). The scanned wavenumbers were in the range of 4000−400 cm^{-1}. TG-FTIR of the hydrochar was performed using simultaneous thermogravimetry (NETZSCH STA 409, Germany) coupled with FTIR (Shimadzu IRAffinity-1s, Japan). Approximately 10 mg of hydrochar was heated from room temperature to 900 °C at the heating rate of 20 °C/min and a N_2 flow rate of 70 mL/min.

RESULTS AND DISCUSSION

Characteristics of Hydrochars. As shown in Figure 1, the yield of SS derivative hydrochar notably decreased from 58.5 to 44.8% at increasing temperatures (from 180 to 240 °C). It is well known that hydrolysis of proteins and polysaccharides is a

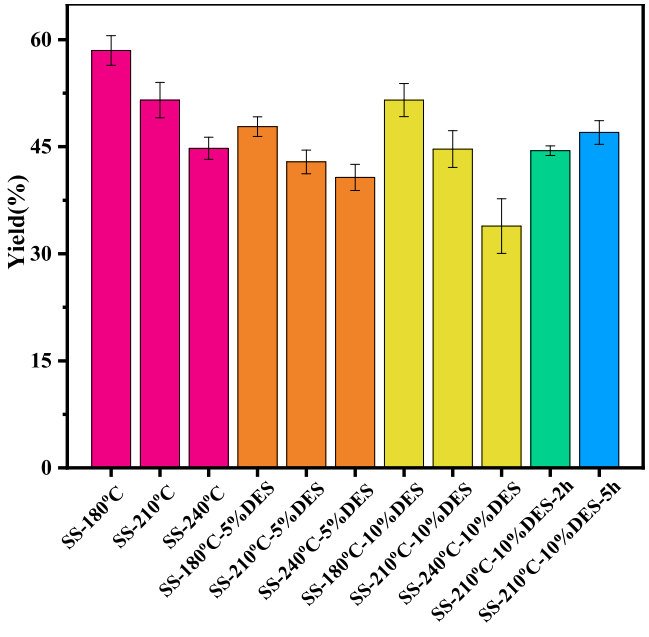

Figure 1. Hydrochar yields.

https://doi.org/10.1021/acssuschemeng.2c00086
ACS Sustainable Chem. Eng. 2022, 10, 4258−4268

key step during HTC of SS, resulting in enhancing the hydrolysis at high temperatures to release more organic matter to the aqueous phase and thus decreasing the yield of hydrochar.[6] In contrast, higher temperatures promote dehydration, deamination, decarboxylation, and thermal decomposition, which improve the degree of coalification, leading to a decrease in the yield of hydrochar.[31] It is known that hydrolysis, dehydration, decarboxylation, and polymerization mainly occur during HTC, leading to a hydrochar.[3] However, the addition of DES could break hydrogen bonds in EPS and the cell wall, promoting the dissolution of organic matter in the aqueous phase and resulting in a decreased yield. When 10% DES was added, the yield at 180 and 210 °C was significantly higher as compared to that obtained by adding 5% DES under otherwise identical conditions. DES catalyzed organic matter dissolution in the aqueous phase to form hydrochar at low temperatures, leading to slightly increased yields. Another possibility was that urea in DES was decomposed and doped organic matter to form N-hydrochar.[32]

After soaking SS in the DES solution for 2 or 5 h, the hydrochar yield slightly increased, indicating that the urea in DES took part in the reaction during soaking by the Maillard reaction, allowing the reaction to take place at very low temperatures. According to Figure 1, temperature is a very important factor during HTC. Additionally, DES played a key role during HTC, including treatment style. In this work, the inorganic matter was not removed. Hence, the solid residue was not really a hydrochar but was still called that for convenience. For high solubility of $ZnCl_2$ and urea, the masses of $ZnCl_2$ and urea were not deducted in the hydrochar.

FTIR analysis of the functional groups of hydrochars under different conditions is depicted in Figure 2. The weak band at

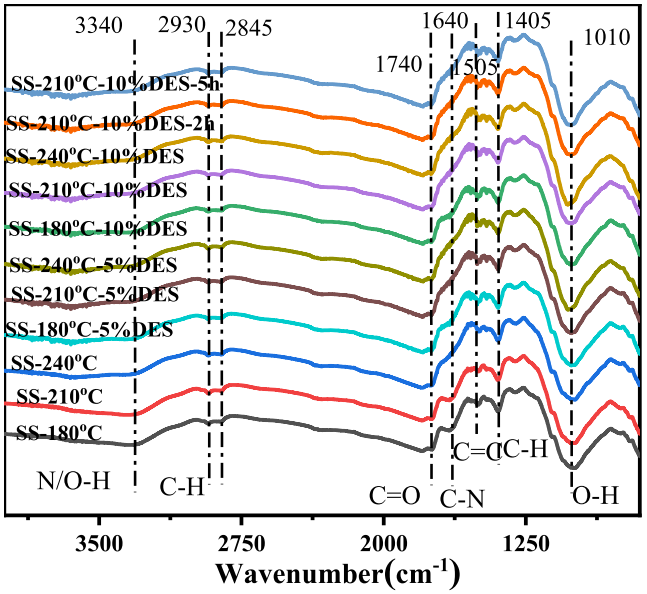

Figure 2. FTIR results of hydrochar.

about 3340 cm^{-1} was attributed to the −N/OH vibration for SS derivative hydrochars containing nitrogen and oxygen. The weak bands at about 2930 and 2850 cm^{-1} were ascribed to the $-CH_2$ stretching vibration. The band located at 1740 cm^{-1} was ascribed to C═O of lipids, indicating that lipids were adsorbed on the surface of hydrochar.[6] The band at 1645 cm^{-1} could be assigned to the stretching vibration of −C═O of the amide group.[33] Another possibility was the C═N vibration in heterocyclic compounds.[34] Significant differences in the profile were found when DES was added. After DES addition or soaking pretreatment, the protein band (1645 cm^{-1}) was very weak (or even disappeared), indicating that DES cleaved the protein structure to form soluble proteins. In other words, soaking pretreatment enhanced the dissolution of the proteins, which probably was a key factor that influenced the HTC process and hydrochar properties. The sharp band located at 1505 cm^{-1} could be ascribed to aromatic ring C═C stretching.[31] The relatively strong band located at 1406 cm^{-1} could be ascribed to the C−H vibration.[31] The band located at 1010 cm^{-1} was due to the stretching of the −C−O−R in polysaccharide or may be attributed to the −Si−O stretching for a large amount of ash in hydrochar.[31] According to FTIR results, it was confirmed that DES disrupted the protein structure to form soluble proteins in the aqueous phase, which would notably influence the HTC process and hydrochar properties.

The results of elemental analysis for hydrochar are listed in Table 1. C, H, N, S, and O contents in hydrochar notably decreased at increasing temperatures, especially C and O. This indicated that parts of proteins and polysaccharides have been transferred into the aqueous phase. Moreover, it indicated an enhanced dehydration and decarboxylation process. When DES was added, the contents of C, H, N, O, and S all decreased in the hydrochar, especially the sample with 10%, indicating that DES can notably promote hydrolysis, dehydration, and decarboxylation during HTC to reduce the content of those elements. On the other hand, FTIR results showed that the amido bond was cleaved after the addition of DES, indicating that polysaccharides were easily dehydrated and decarboxylated after the dissolution of proteins. For the 5% DES, S can be found in the hydrochar, indicating that proteins were still partially retained in the SS during HTC and were not dissolved completely. When 10% DES was added, almost no S could be found in the hydrochar, which shows that protein dissolution enhanced on increasing the DES. When DES soaking pretreatment was carried out, it was found that the elemental content slightly increased in the hydrochar, indicating that the Maillard reaction probably caused the reaction to take place at low temperatures.[35] The Maillard reaction between dissolution proteins in the aqueous phase and urea in DES with polysaccharides took place at low temperatures, forming relatively large molecular compounds that increased the elemental content in the hydrochar.

On the other hand, DES was not completely removed under HTC conditions. he addition of DES induced extensive disruption in SS so that proteins were released to the aqueous phase, changing the elemental composition of hydrochars. In this sense, DES was confirmed to play a role in protein transfer during HTC.

Figure 3 depicts the van Krevelen diagram calculated from Table 1, which presents the H/C vs O/C atomic ratios. The main reactions during HTC of SS included decarboxylation, demethylation, and dehydration. Dehydration was enhanced in the lower-temperature range, while the O/C increased at 240 °C (probably related to the Diels−Alder reaction, where a precursor containing the oxygen atom brought oxygen to the hydrochar). When 5% DES was added, O/C and H/C both increased as compared to the reaction in the absence of DES. When 10% DES was added, it was found that as the temperature increased, the dehydration was enhanced. When

https://doi.org/10.1021/acssuschemeng.2c00086
ACS Sustainable Chem. Eng. 2022, 10, 4258−4268

Table 1. Elemental Analysis of Hydrochar Samples

samples	N	C	H	S	O	HHV (MJ/kg)
SS-180 °C	3.47	20.44	4.17	0.52	19.15	9.49
SS-210 °C	3.15	19.47	3.89	0.33	17.54	9.04
SS-240 °C	2.25	16.97	3.39	0.25	15.64	7.80
SS-180 °C-5%DES	2.83	16.74	3.59	0.59	16.40	7.92
SS-210 °C-5%DES	2.13	14.35	3.18	0.52	14.35	6.88
SS-240 °C-5%DES	1.80	13.50	2.81	0.50	12.92	6.31
SS-180 °C-10%DES	2.57	15.55	3.28	0.47	15.00	7.31
SS-210 °C-10%DES	1.93	13.36	2.75	<0.10	13.23	6.08
SS-240 °C-10%DES	1.68	12.45	2.41	<0.10	11.89	5.52
SS-210 °C-10%DES-2h	1.99	13.58	2.89	<0.10	14.24	6.18
SS-210 °C-10%DES-5h	1.99	13.58	2.89	<0.10	14.36	6.15

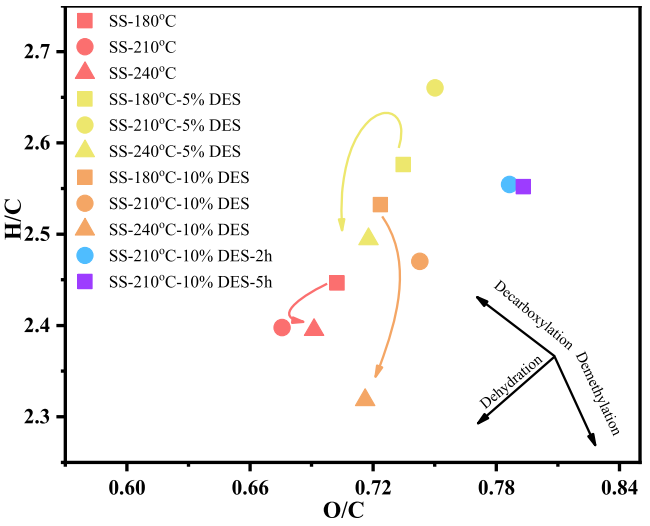

Figure 3. Van Krevelen diagram of hydrochars with and without FN.

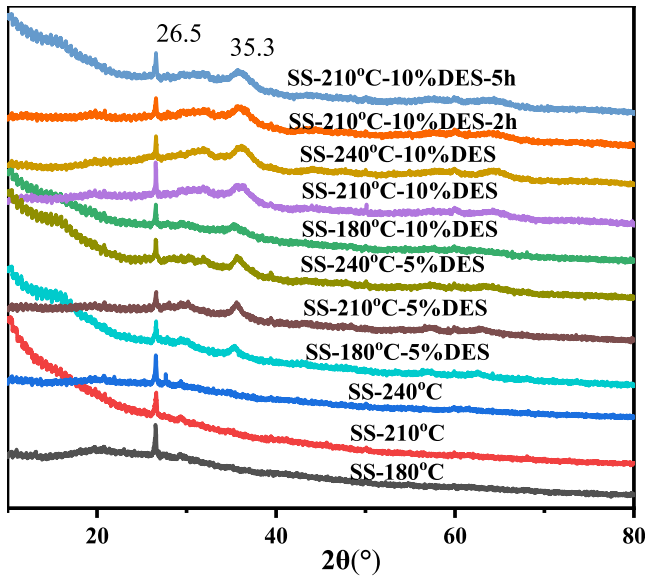

Figure 4. XRD patterns of the different hydrochars.

SS was soaked for 2 and 5 h in the DES solution, the O/C and H/C were higher than those without DES and 5% DES under the same HTC conditions. The difference in the O/C and H/C of samples with the DES shifting to a high value was probably caused by $ZnCl_2$. In the present paper, hydrochar was not rinsed, indicating that $ZnCl_2$ was retained (probably as Cl^- adsorbed on the surface of the hydrochar), resulting in other inorganic matter also being adsorbed on the surface via a hydrogen bond. In our previous work, the inorganic matter was demonstrated to adsorb on the surface of the hydrochar.[8] According to Figure 3, it was confirmed that DES was a key factor, especially in protein "dissolution". After disrupting the protein structure, and according to the thermal decomposition reaction and the Maillard reaction, deamination of SS could also be enhanced. Certainly, decarboxylation and dehydration were enhanced.

To analyze the structure of the hydrochar, XRD is used for the analysis of the crystalline nature listed in Figure 4. The sharp peak at 26.5° ascribed to the amorphous carbon in SS-derived hydrochars could also belong to SiO_2 crystallites of SS containing a large amount of ash. Another peak was noted at 35.3°. The typical peak of $ZnCl_2$ is 16.3°,[36] and as seen in Figure 4, it is absent, indicating that $ZnCl_2$ was transferred into another Zn species. It is known that during HTC of SS, deamination of proteins takes place, which increases the pH of the aqueous phase for NH_4^+ formation. Under alkaline conditions, Zn^{2+} can form $Zn(OH)_2$, as a locally high concentration of bases favors the formation of $Zn(OH)_2$. However, the typical peak of $Zn(OH)_2$ located at 20.86° cannot be found, indicating that $Zn(OH)_2$ did not exist in the hydrochar. The peak located at 35.3° probably was ZnO since very weak peaks located at 32.3, 47.8, 56.7, and 62.9° could be found.[37] However, the typical peaks of ZnO were 32.3, 34.9, 36.6, and 47.8°. Hence, according to the sharp peak and weak peaks, the maximum possibility was $Zn_5(OH)_8Cl_2{\cdot}H_2O$ derivative compounds.[38] After HTC, the $Zn_5(OH)_8Cl_2{\cdot}H_2O$ initial thermal decomposition occurred at about 150 °C to β-Zn(OH)C1 and then further decomposed to give the present results, different from that of ZnO (also explaining the high H/C and O/C values in DES-treated samples).

To further analyze the role of DES in hydrochar formation, the surface morphological structure of hydrochar was scanned by SEM. The difference in samples is shown in Figure 5. Small pores could be observed on the surface of hydrochar without DES. However, the surface was relatively rough, indicating that dehydration, decarboxylation, and deamination occurred in a limited way relatively. When 5% DES was added, pores could also be observed on the surface of hydrochar; however, the surface was relatively smooth, indicating that the hydrolysis process of proteins and polysaccharides was enhanced and then the hydrolysate was polymerized to form hydrochar. It implied that DES has a positive effect on HTC of SS. When 10% DES was added, pores could still be observed on the surface, and they became small. It showed that the 10% DES

https://doi.org/10.1021/acssuschemeng.2c00086
ACS Sustainable Chem. Eng. 2022, 10, 4258−4268

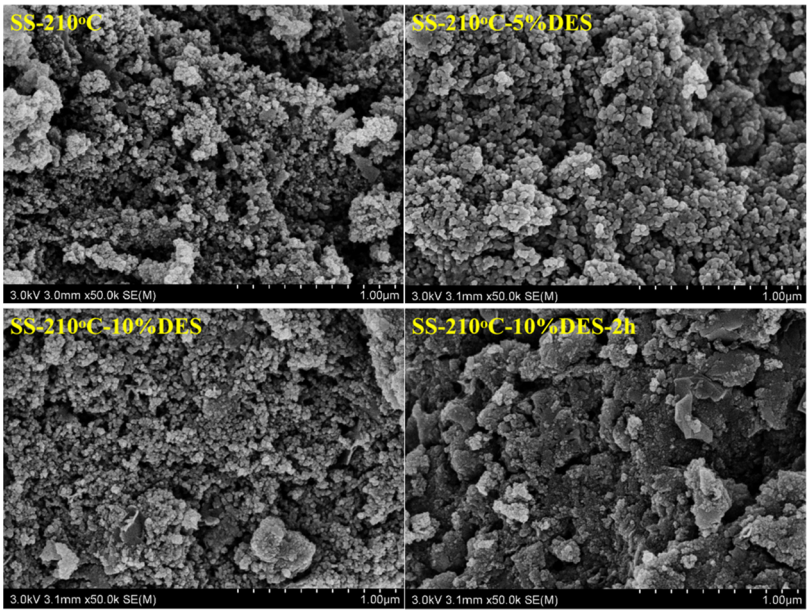

Figure 5. SEM of hydrochars at 210 °C (with and without DES).

dissolved more organic matter; especially, proteins and more organic matter transferred into the aqueous phase and formed more hydrochar, resulting in the formation of small pores on the surface of hydrochar.

On the other hand, large particles could be observed on the surface. After soaking for 5 h, the particles of hydrochar were found to agglomerate, with a very rough surface in the hydrochar. At the same time, crystals could be found, indicating that the inorganic matter went through crystallization. Small particles were also observed on the surface, indicating hydrochar formation from the aqueous phase. Large pores on the surface of the hydrochar probably implied that polysaccharide hydrolysis could be enhanced to dissolve more polysaccharides after protein dissolution. Comparing with and without soaking, soaking benefited organic matter hydrolysis and DES was indeed effective in the HTC process. From the above analysis, the DES was found to have enhanced the hydrolysis process of the biopolymer, due to which SS could enhance the biopolymer solubility, forming low-molecular-weight organic matter.

On the other hand, more organic matter dissolving in the aqueous phase polymerized during HTC, forming solid particles on the surface. Hence, the number of pores decreased on increasing the fraction of DES. DES addition durign HTC enhanced dissolution, causing dehydration, deamination, and decarboxylation reactions leading to pore formation. These reactions facilitated N and S element removal from SS, resulting in low N and S elemental contents in hydrochars.

Characteristics of the Liquid Phase. To analyze the properties of the aqueous phase, the TOC value of the aqueous phase was measured first. The TOC was tested under different conditions, and the results are listed in Figure 6.

From 180 to 210 °C, the TOC value of the aqueous phase increased with temperature increasing, indicating that high temperature promoted organic matter in SS hydrolysis and thermal decomposition to release low-molecular-weight organic matter to the aqueous phase. When the temperature increased to 240 °C, the TOC value slightly decreased, indicating that the dehydration, deamination, and decarboxylation were enhanced to release CO_2 and H_2O. When 5% DES was added, compared to that without DES, the TOC value slightly increased at 180 °C and notably decreased at 210 °C. It indicated that at low temperatures, DES promoted protein "dissolution" of SS to release soluble proteins to the aqueous phase. TOC reduction was mainly caused by deamination and decarboxylation to release NH_3 and CO_2. When the temperature was increased to 240 °C, the TOC had almost no change compared to without DES. It probably was the reaction between NH_4^+ and polysaccharide, which formed N-organic matter and resulted in an increase in the TOC.[39] When 10% DES was added, compared with 5%, the TOC value increased in a stepwise manner, indicating that protein "dissolution" was enhanced and polysaccharides could also be enhanced. When SS was soaked in DES solution for 2 and 5 h, the TOC value slightly increased compared to that with 10%

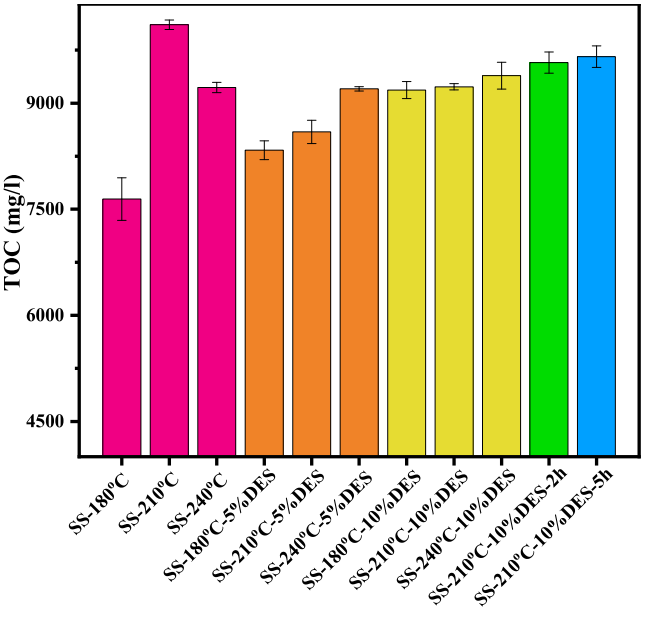

Figure 6. TOC results of the aqueous phase.

https://doi.org/10.1021/acssuschemeng.2c00086
ACS Sustainable Chem. Eng. 2022, 10, 4258−4268

DES. It indicated that more proteins were transferred into the aqueous phase after soaking, leading to an increase in the TOC value. Comparing with and without soaking, it was found that soaking pretreatment was beneficial to organic matter "dissolution" and hydrolysis because after directly adding DES to SS under the HTC condition, deamination increased the pH value, leading to the formation of $Zn_5(OH)_8Cl_2{\cdot}H_2O$. It destroyed the DES system and inhibited DES dissolution in proteins, resulting in the TOC value decreasing. According to TOC results, it indicated that temperature and DES were sensitive factors, especially DES.

NH_3-N and TN values were all further analyzed, and results are listed in Figure 7. With increasing temperature, NH_3-N values increased in a stepwise manner during HTC of SS in the range of 180−240 °C. The NH_3-N value increase was mainly caused by deamination of labile amides under HTC conditions to form NH_4^+.[8] It indicated that with temperature increasing, hydrolysis of proteins was enhanced to facilitate deamination. Paneque et al. found that NH_3-N was mainly related to amino acid thermal decomposition during HTC.[40] Actually, a low fraction of amino acids in the aqueous phase of HTC for SS can be found.[41] Hence, deamination of labile amides was the main reason for the increase in NH_3-N values. When DES was added, the NH_3-N values notably increased. When 5% DES was added, the NH_3-N values notably increased, especially at 220 and 240 °C. Compared to the aqueous phase without DES, the NH_3-N value was higher than the deamination of labile amides without DES and urea-produced NH_4^+, indicating that after DES addition, more labile amides from SS were transferred into the aqueous phase and carried out deamination to form more NH_4^+.

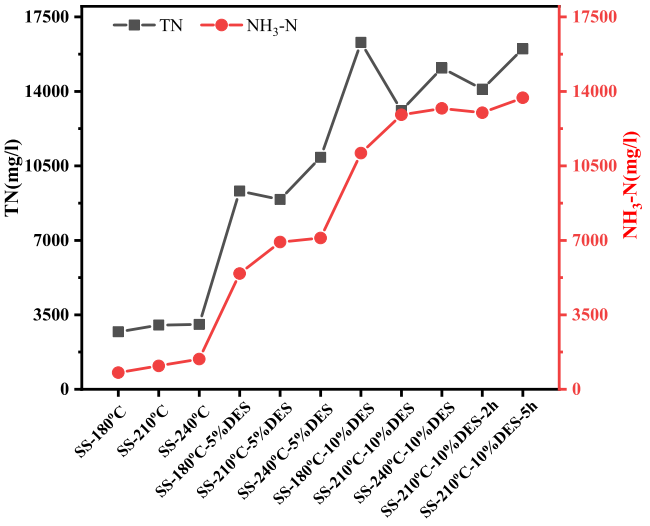

Figure 7. NH_3-N and TN results of the aqueous phase.

DES is an effective method to transfer more proteins into the aqueous phase. When 10% DES was added, the NH_3-N value also notably increased. A probable key reason was the amount of urea increasing. Certainly labile amides also contributed to the NH_3-N value increasing. After soaking for 2 and 5 h, the NH_3-N value in the aqueous phase was slightly higher than that of 10% DES, indicating that soaking pretreatment was beneficial to organic matter "dissolution" and hydrolysis, especially under HTC conditions, in good agreement with TOC results. TN values are also listed in Figure 7. TN increased in a stepwise manner in the range of 180−240 °C, mainly caused by the hydrolysis of proteins under HTC conditions to form soluble proteins and other N-organic matter. When 5% DES was added, TN was fluctuant in the range of 180−240 °C. When the temperature was increased to 210 from 180 °C, the TN value slightly decreased, and it notably increased again when the temperature was increased to 240 °C. It implied that the Maillard reaction that took place during HTC for nitrogen in the aqueous phase can only transfer into the solid phase to form hydrochar. When 10% DES was added, similar results were found, and the change was significant, pointing to an enhancement of the Maillard reaction at this temperature (or more soluble proteins took part in the reaction between soluble proteins and polysaccharides). Although more soluble proteins can be found at 240 °C, polysaccharides were further hydrolyzed and dehydrated to form macromolecular compounds and small molecular compounds, resulting in difficulties in reacting with proteins. During HTC, almost no N_2 in nitrogen species distribution was formed. Hence, TN at 240 °C increased again. After soaking for 2 and 5 h, the TN value in the aqueous phase was notably higher than that of 10% DES, indicating that soaking pretreatment was beneficial for protein "dissolution". It was confirmed that after soaking, more proteins could be transferred into the aqueous phase under HTC conditions. According to NH_3-N and TN results, it was confirmed that DES could notably dissolve proteins in an aqueous phase and change the SS floc structure properties, which would influence hydrochar properties.

To further analyze soluble protein change under HTC conditions, 3D-EEM was used to analyze aqueous phase properties. Regions I, II, III, and V are aromatic protein-like I, aromatic protein-like II, fulvic acid-like, and humic acid-like substances, respectively. Region IV corresponded to protein-like, tryptophan, tyrosine and related N-containing compounds. To demonstrate the change of proteins in the aqueous phase when DES was added, the aqueous phase with and without DES was selected, as listed in Figure 8. The typical aqueous phase samples were analyzed and are listed in Figure S1. It was found that with increasing temperature, the overall intensity decreased, especially at 240 °C, indicating that thermal decomposition of proteins was enhanced, indicating more NH_4^+ formation. It was in agreement with the NH_3-N

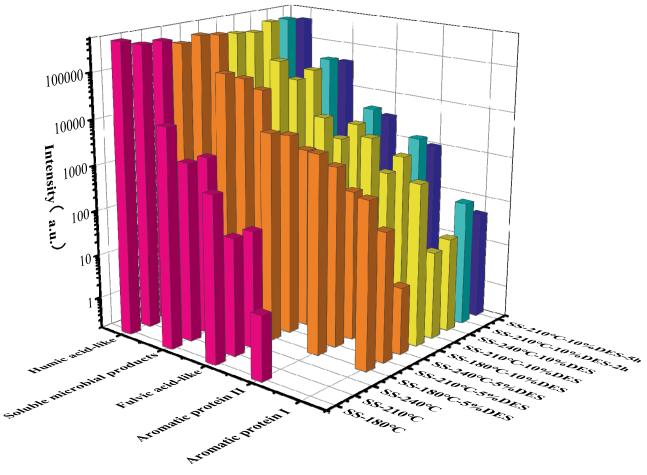

Figure 8. Intensity of 3D-EEM for the aqueous phase with and without DES.

https://doi.org/10.1021/acssuschemeng.2c00086
ACS Sustainable Chem. Eng. 2022, 10, 4258−4268

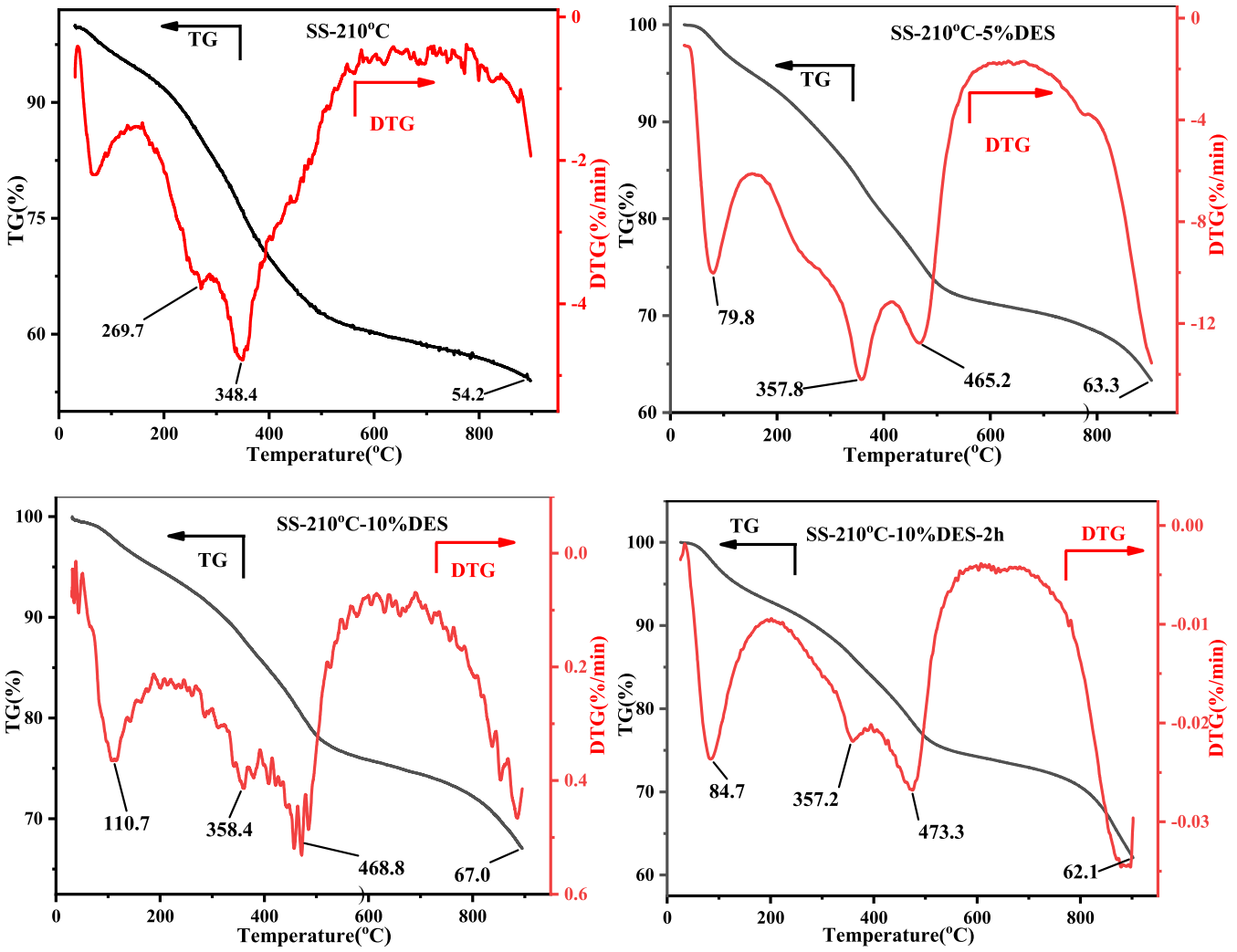

Figure 9. TG-DTG results of hydrochars.

results. When 5% DES was added, the intensity of proteins notably increased under the same conditions, except for the humic acid-like slight decrease. It implied that DES notably promoted protein hydrolysis. With the temperature increasing, the intensity of proteins decreased in a stepwise manner, except for the humic acid-like fluctuant, indicating that deamination of proteins took place at high temperatures. It was in agreement with NH_3-N results. When 10% DES was added, the intensity notably fluctuated compared to that of with 5%. It indicated that proteins were transferred into the aqueous phase from SS when 10% DES was added; then, deamination, thermal decomposition, and Maillard reaction occurred at the same time, and which one dominated during HTC depended on the HTC temperature. Hence, it caused the intensity to be fluctuant. After soaking for 2 and 5 h, the intensity was notably higher than that of 10% DES, indicating that soaking pretreatment was beneficial to protein "dissolution". It was in line with FTIR, TOC, and TN results. On the other hand, it was found that with the soaking time prolonging, the intensity notably decreased, indicating that deamination took place during HTC, which decreased the intensity. It was in line with TN and NH_3-N results. It was confirmed that more proteins can be transferred into the aqueous phase under HTC conditions after soaking. Combined with TOC, TN, and NH_3-N results, it was confirmed that under HTC conditions, DES can notably dissolve proteins in the aqueous phase and change the aqueous phase properties and SS floc structure properties.

Thermal Decomposition Characteristic of Hydrochars. To investigate the thermal decomposition properties of hydrochars, the TG-DTG of hydrochars with 20 °C/min using N_2 as the inert atmosphere was conducted from room temperature to 900 °C (Figure 9). The hydrochar produced at 210 °C showed two peaks at 269.7 and 348.4 °C. These were related to the thermal decomposition of proteins[42] and polysaccharides,[43] respectively. The weak peak at ca. 100 °C was attributed to the removal of physisorbed water. The residue was 54.2%. When 5% DES was added, the weak peak near 100 °C was also observed. The sharp peak shifted to a high temperature (357.8 °C), indicating that after DES addition volatiles were removed from SS. From the above results, the main difference upon DES addition relates to partial proteins being transferred into the aqueous phase, indicating that proteins can form heavy compounds by the Maillard reaction and increase the thermal decomposition temperature. On the other hand, the hydrogen-bond network between proteins and polysaccharides was disrupted by DES, resulting in polysaccharide hydrolysis and dehydration to enhance carbonization and thus increase the thermal decomposition temperature. It is well known that the peak at

https://doi.org/10.1021/acssuschemeng.2c00086
ACS Sustainable Chem. Eng. 2022, 10, 4258−4268

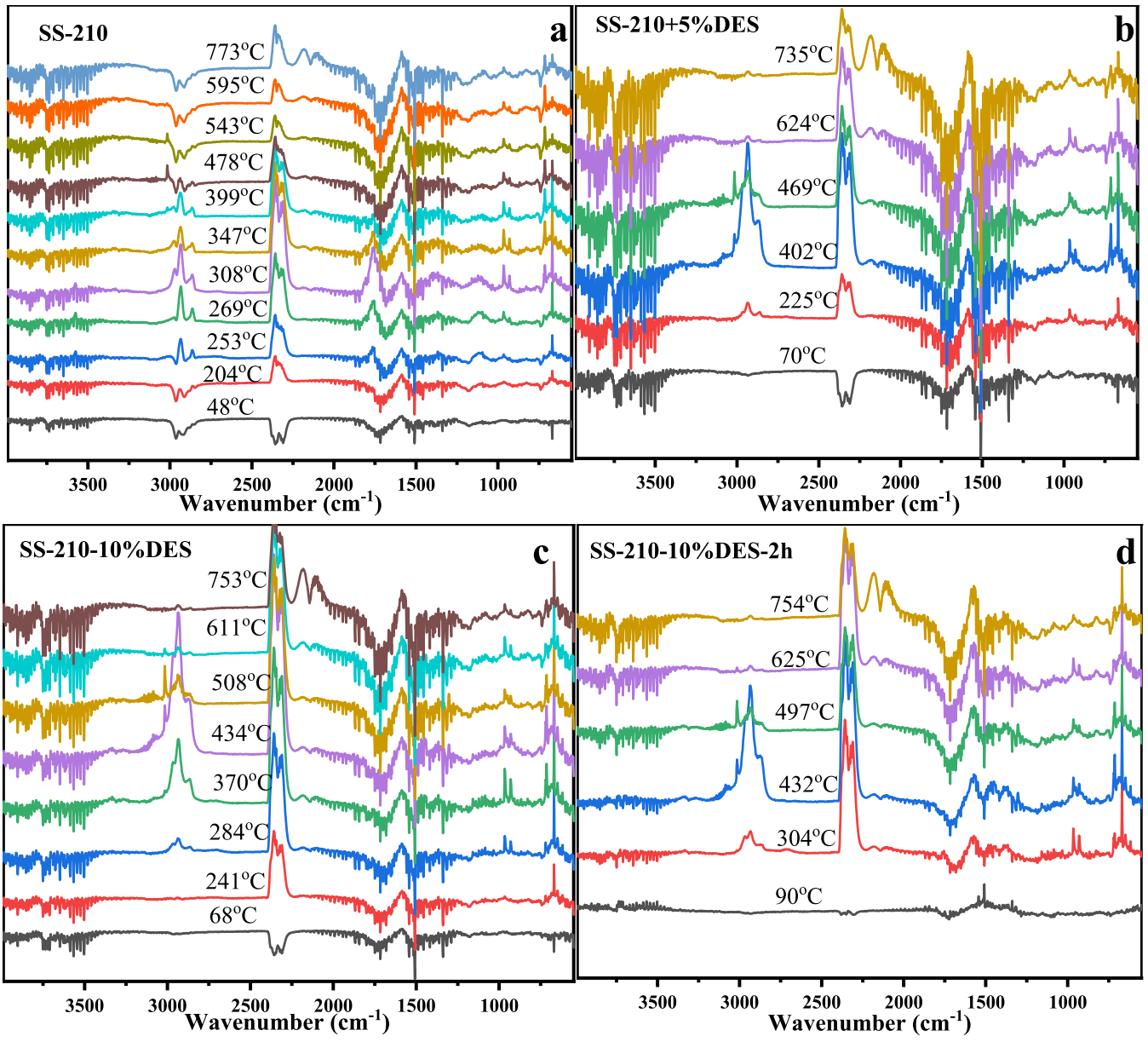

Figure 10. TG-FTIR spectra of hydrochars under different conditions.

ca. 430 °C was possibly associated with the thermal decomposition of residual lignin to fixed carbon[44] or humic substances.[45] The sharp peak located at 465.2 °C indicated the high degree of carbonization (shifted to high for thermal decomposition of fixed carbon or humic substances). In other words, disruption of the SS floc structure and "dissolved" proteins can benefit polysaccharide carbonization during HTC, increasing the thermal decomposition temperature. Thermal decomposition peaks were split when 10% DES was added. The weak peak at ca. 110 °C was also detected. After 200 °C, small thermal decomposition peaks can be found, probably related to protein thermal decomposition to release NH_3. These results indicated that 10% DES can notably dissolve proteins in the aqueous phase from SS as well as proteins undergoing Maillard chemistry/adsorption on the surface, resulting in persistent thermal decomposition to form the observed split peaks. The first split peak appeared at 358.4 °C. The second main split peak appeared at ca. 468.8 °C. The residue was 67.0%. The appearance of split peaks indicated that 10% DES can dissolve more proteins in the aqueous phase, while limited HTC time (1 h) originated a limited dissolution of proteins. After soaking for 2 h in DES, a smooth thermal decomposition curve was observed. The first thermal decomposition peak (348.4 °C) shifted to 358.4 °C after DES addition, which was ascribed to polysaccharide thermal decomposition. DES promoted polysaccharide carbonization for high thermal decomposition temperature. As compared to without the soaking treatment, the thermal decomposition temperature of the hydrochar for the second peak was increased by about 8 °C, indicating the higher degree of carbonization (the peak can be ascribed to the fixed carbon or humic substances). The residue was 62.1%. From TG-DTG results, DES was further confirmed to promote protein dissolution and the increased carbonization degree of polysaccharides. It also promoted the reaction between proteins and polysaccharides to form heavy compounds although relatively limited under current investigated conditions.

https://doi.org/10.1021/acssuschemeng.2c00086
ACS Sustainable Chem. Eng. 2022, 10, 4258−4268

To further investigate the thermal decomposition characteristics, TG-FTIR was investigated at 20 °C/min in a N_2 atmosphere, as shown in Figure 10. The main species included CO_2 (a sharp doublet band at 2400−2250 cm^{-1} and a low-intensity band at 670 cm^{-1}), C═O (1750 cm^{-1}), and C−O−C (approximately 1500 cm^{-1}). The band located at 4000−3400 cm^{-1} was attributed to O/N−H bonds (stretching vibrations) from H_2O/NH_3.[45,46] According to Figure 10, the thermal decomposition of hydrochar showed that decarboxylation took place after 200 °C, indicating that the surface of hydrochar contains −COOH groups. The signal of NH_3 was very strong (near 3500 cm^{-1}). Alkane signals could be observed after 250 °C, indicating that the carbon skeleton of hydrochar began to break down. After 270 °C, aromatic compounds could be detected (960, 930, and 710 cm^{-1}). After 310 °C, the signal of aromatic compounds became more evident. After 350 °C, the signal of CO could be detected (2140 cm^{-1}), probably due to thermal decomposition of lipids adsorbed on the surface of hydrochar.[47] After 400 °C, there was complete thermal decomposition of lipids since the band (1760 cm^{-1}) disappeared. It indicated that lipids in hydrochar were short-chain lipids since the thermal decomposition temperature of plant oil exceeded 400 °C. After 550 °C, the release of CO_2 and aromatic compounds became weak.

The addition of DES brought relevant changes in the decomposition profile. After 225 °C, the weak signals of alkane NH_3, CO_2, and aromatic compounds were found, indicating that the initial thermal decomposition temperature shifted to high. After 400 °C, the signals of alkane, NH_3, CO_2, and aromatic compounds became strong. It indicated that compared to hydrochar without DES, the heavy compounds formed when DES was added and light compounds were removed. After 470 °C, the signal of alkane became weak but that of aromatic compounds became strong, indicating that the degree of carbonization became strong when DES was added. After 630 °C, almost no signal of aromatic compounds and alkane could be found, and the signal of CO became strong. No lipid signal could be found, indicating that DES could remove lipids during HTC. When 10% DES was added, after 240 °C, a weak signal of CO_2 could be found, indicating that decarboxylation took place. The initial temperature of this hydrochar was higher than that of with 5% DES, indicating that DES can remove volatile compounds in hydrochar. After 285 °C, a weak signal of alkane and aromatic compounds could be found. It implied that the reaction of thermal decomposition became slowly accelerated. After 370 °C, a strong signal could be found, which became very strong at 440 °C. After 510 °C, the signal of aromatic compounds and alkane became weak. However, the signal of −COOH was still very strong, indicating that DES promoted polysaccharide carbonization for carboxylic acid formation during HTC of polysaccharides. After 610 °C, the signals of aromatic compounds and alkane also disappeared. When DES soaking was carried out, after 305 °C, weak signals of alkane and aromatic compounds could be found. It implied that the reaction of thermal decomposition became slowly accelerated. When the temperature was increased to 430 °C, the signals of alkane and aromatic compounds became very strong and then became weak with the temperature increasing. After 500 °C, the signals of alkane and aromatic compounds became weak, and the signal of −COOH was still intense. After 620 °C, the signals of aromatic compounds and alkane also disappeared. According to TG-FTIR results, it was confirmed that DES could notably dissolve proteins and lipids during HTC of SS. The lipids in SS were short-chain triglycerides. The HTC of polysaccharides was enhanced, increasing the degree of carbonization. With DES addition, volatile compounds could be removed, resulting in an initial temperature increase. Hence, TG-FTIR provided another view to show the influence of DES on HTC of SS.

To further analyze the thermal decomposition properties of hydrochar, Py-GC/MS was used to analyze pyrolysis components (Figure 11). The main compounds are listed in Tables S1−S4. The notable differences are listed in Figure 11. First, a large amount of CO_2 could be found in hydrochars, indicating more −COOH groups on the surface of hydrochars. It was in line with TG-FTIR results. Compared to results without DES, more alkanes and alkenes could be found when DES was added, indicating that DES notably promoted polysaccharide transformations and inhibited the Maillard reaction to form a low content of N-organic compounds during HTC of SS.

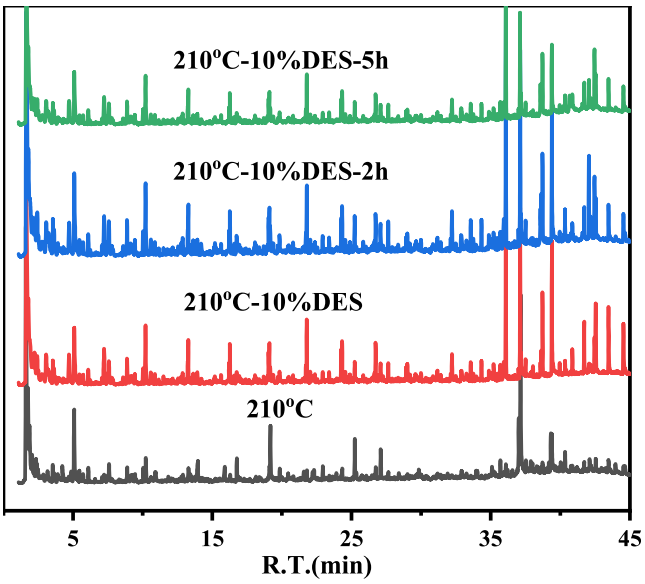

Figure 11. Py-GC/MS detection of gas products evolved from hydrochar.

On the other hand, proteins were also probably the source of alkanes and alkenes. When DES was not added, the main compounds were heavy fatty acids. When 10% DES was added, the main compounds included heavy fatty acids, long-chain alkanes, and heavy N-organic matter. It indicated that proteins probably carried out deamination and decarboxylation to form long-chain alkanes. The Maillard reaction was the main reaction that formed heavy N-organic matter. When SS was soaked in the DES solution for 2 and 5 h, it was seen that more N-organic matter was found in Py-GC-MS results. Soaking pretreatment consequently promoted N-organic matter formation.

CONCLUSIONS

DES-assisted HTC was successfully developed and investigated in detail. DES can notably dissolve proteins and lipids during HTC of SS. Lipids in SS were short-chain triglycerides. The HTC of polysaccharides was enhanced to increase the degree of carbonization as thermal decomposition temperatures shifted to high temperatures. The key role of DES in SS

https://doi.org/10.1021/acssuschemeng.2c00086
ACS Sustainable Chem. Eng. 2022, 10, 4258−4268

during HTC was protein dissolution, promoting carbonization of polysaccharides, the Maillard reaction, deamination, and decarboxylation of proteins. $ZnCl_2$ during HTC was probably converted into a mixture of β-Zn(OH)C1 and ZnO. A low-nitrogen-content hydrochar could be obtained as a clean solid fuel.

■ ASSOCIATED CONTENT

Supporting Information

The Supporting Information is available free of charge at https://pubs.acs.org/doi/10.1021/acssuschemeng.2c00086.

Details of the main compounds from Py-GC-MS and the typical aqueous phase samples analyzed by 3D-EEM (PDF)

■ AUTHOR INFORMATION

Corresponding Authors

Zhixiang Xu − *School of Energy and Power Engineering, Jiangsu University, Zhenjiang 212013, China;* orcid.org/0000-0003-3944-3944; Email: xuzx@ujs.edu.cn

Shiyong Wu − *State Key Laboratory of High-efficiency Utilization of Coal and Green Chemical Engineering, College of Chemistry and Chemical Engineering, Ningxia University, Yinchuan 750021, China*; Email: wsy@ecust.edu.cn

Rafael Luque − *Departamento de Quimica Organica, Campus de Rabanales, Edificio Marie Curie (C-3), E14014 Cordoba, Spain; Peoples Friendship University of Russia (RUDN University), Moscow 117198, Russian Federation;* orcid.org/0000-0003-4190-1916; Email: rafael.luque@uco.es

Authors

Xueqin Ma − *School of Energy and Power Engineering, Jiangsu University, Zhenjiang 212013, China*

Junjie Liao − *State Key Laboratory of Clean and Efficient Coal Utilization and Key Laboratory of Coal Science and Technology, Ministry of Education, Taiyuan University of Technology, Taiyuan 030024, China;* orcid.org/0000-0003-0983-4469

Sameh M. Osman − *Chemistry Department, College of Science, King Saud University, Riyadh 11451, Saudi Arabia*

Complete contact information is available at: https://pubs.acs.org/10.1021/acssuschemeng.2c00086

Notes

The authors declare no competing financial interest.

■ ACKNOWLEDGMENTS

This research was supported by the State Key Laboratory of Clean and Efficient Coal Utilization and the Key Laboratory of Coal Science and Technology, Ministry of Education (China). The research was also supported by the State Key Laboratory of High-efficiency Utilization of Coal and Green Chemical Engineering (China). This project was funded by the Researchers Supporting Project number (RSP-2021/405), King Saud University, Riyadh, Saudi Arabia. This publication was supported by RUDN University Strategic Academic Leadership Program (R. Luque). R. Luque gratefully acknowledges funding for Open Access charges to Universidad de Córdoba/CBUA.

■ REFERENCES

(1) Tan, X.; Xie, G. J.; Nie, W. B.; Xing, D. F.; Liu, B. F.; Ding, J.; Ren, N. Q. High value-added biomaterials recovery from granular sludge based wastewater treatment process. *Resour., Conserv. Recycl.* **2021**, *169*, No. 105481.

(2) Feng, C. J.; Welles, L.; Zhang, X. D.; Pronk, M.; de Graaff, D.; van Loosdrecht, M. Stress-induced assays for polyphosphate quantification by uncoupling acetic acid uptake and anaerobic phosphorus release. *Water Res.* **2020**, *169*, No. 115228.

(3) Wang, T. F.; Zhai, Y. B.; Zhu, Y.; Li, C. T.; Zeng, G. M. A review of the hydrothermal carbonization of biomass waste for hydrochar formation: Process conditions, fundamentals, and physicochemical properties. *Renewable Sustainable Energy Rev.* **2018**, *90*, 223−247.

(4) Seviour, T.; Derlon, N.; Dueholm, M. S.; Flemming, H. C.; Girbal-Neuhauser, E.; Horn, H.; Kjelleberg, S.; van Loosdrecht, M. C. M.; Lotti, T.; Malpei, M. F.; Nerenberg, R.; Neu, T. R.; Paul, E.; Yu, H. Q.; Lin, Y. M. Extracellular polymeric substances of biofilms: Suffering from an identity crisis. *Water Res.* **2019**, *151*, 1−7.

(5) Xu, Z. X.; Deng, X. Q.; Zhang, S.; Shen, Y. F.; Shan, Y. Q.; Zhang, Z. M.; Luque, R.; Duan, P. G.; Hu, X. Benign-by-design N-doped carbonaceous materials obtained from the hydrothermal carbonization of sewage sludge for supercapacitor applications. *Green Chem.* **2020**, *22*, 3885−3895.

(6) Xu, Z. X.; Song, H.; Li, P. J.; Zhu, X.; Zhang, S.; Wang, Q.; Duan, P. G.; Hu, X. A new method for removal of nitrogen in sewage sludge-derived hydrochar with hydrotalcite as the catalyst. *J. Hazard. Mater.* **2020**, *398*, No. 122833.

(7) Xu, Z. X.; Song, H.; Li, P. J.; He, Z. X.; Wang, Q.; Wang, K.; Duan, P. G. Hydrothermal carbonization of sewage sludge: Effect of aqueous phase recycling. *Chem. Eng. J.* **2020**, *387*, No. 123410.

(8) Xu, Z. X.; Shan, Y. Q.; Zhang, Z.; Deng, X. Q.; Yang, Y.; Luque, R.; Duan, P. G. Hydrothermal carbonization of sewage sludge: effect of inorganic salts on hydrochar's physicochemical properties. *Green Chem.* **2020**, *22*, 7010−7022.

(9) Leng, L. J.; Yang, L. H.; Leng, S. Q.; Zhang, W. J.; Zhou, Y. Y.; Peng, H. Y.; Li, H.; Hu, Y. C.; Jiang, S. J.; Li, H. L. A review on nitrogen transformation in hydrochar during hydrothermal carbonization of biomass containing nitrogen. *Sci. Total Environ.* **2021**, *756*, No. 143679.

(10) Wu, B. R.; Dai, X. H.; Chai, X. L. Critical review on dewatering of sewage sludge: Influential mechanism, conditioning technologies and implications to sludge re-utilizations. *Water Res.* **2020**, *180*, No. 115912.

(11) Gao, N. B.; Kamran, K.; Quan, C.; Williams, P. T. Thermochemical conversion of sewage sludge: A critical review. *Prog. Energy Combust. Sci.* **2020**, *79*, No. 100843.

(12) Wang, H.; Xiao, K. K.; Yang, J. K.; Yu, Z. C.; Yu, W. B.; Xu, Q.; Wu, Q. X.; Liang, S.; Hu, J. P.; Hou, H. J.; Liu, B. C. Phosphorus recovery from the liquid phase of anaerobic digestate using biochar derived from iron-rich sludge: A potential phosphorus fertilizer. *Water Res.* **2020**, *174*, No. 115629.

(13) Nguyen, V. K.; Chaudhary, D. K.; Dahal, R. H.; Trinh, H. N.; Kim, J.; Chang, S. W.; Hong, Y.; Duong Duc, L.; Cuong Nguyen, X.; Hao Ngo, H.; Chung, W. J.; Duc Nguyen, D. Review on pretreatment techniques to improve anaerobic digestion of sewage sludge. *Fuel* **2021**, *285*, No. 119105.

(14) Ma, X. Q.; Liao, J. J.; Chen, D. B.; Xu, Z. X. Hydrothermal carbonization of sewage sludge: Catalytic effect of Cl^- on hydrochars physicochemical properties. *Mol. Catal.* **2021**, *513*, No. 111789.

(15) Yu, W. B.; Wen, Q. Q.; Yang, J. K.; Xiao, K. K.; Zhu, Y. W.; Tao, S. Y.; Lv, Y.; Liang, S.; Fan, W.; Zhu, S. Y.; Liu, B. C.; Hou, H. J.; Hu, J. P. Unraveling oxidation behaviors for intracellular and extracellular from different oxidants (HOCl vs. H_2O_2) catalyzed by ferrous iron in waste activated sludge dewatering. *Water Res.* **2019**, *148*, 60−69.

(16) Chen, K.; Liu, J. X.; Huang, S. M.; Mei, M.; Chen, S.; Wang, T.; Li, J. P. Evaluation of the combined effect of sodium persulfate and thermal hydrolysis on sludge dewatering performance. *Environ. Sci. Pollut. Res.* **2021**, *28*, 7586−7597.

(17) Ning, H.; Zhai, Y. B.; Li, S. H.; Liu, X. M.; Wang, T. F.; Wang, B.; Liu, Y. L.; Qiu, Z. Z.; Li, C. T.; Zhu, Y. Fe(II) activated persulfate assisted hydrothermal conversion of sewage sludge: Focusing on nitrogen transformation mechanism and removal effectiveness. *Chemosphere* **2020**, *244*, No. 125473.
(18) Wang, X. W.; Shen, Y.; Liu, X. C.; Ma, T. F.; Wu, J.; Qi, G. X. Fly ash and H_2O_2 assisted hydrothermal carbonization for improving the nitrogen and sulfur removal from sewage sludge. *Chemosphere* **2022**, *290*, No. 133209.
(19) Hansen, B. B.; Spittle, S.; Chen, B.; Poe, D.; Zhang, Y.; Klein, J. M.; Horton, A.; Adhikari, L.; Zelovich, T.; Doherty, B. W.; Gurkan, B.; Maginn, E. J.; Ragauskas, A.; Dadmun, M.; Zawodzinski, T. A.; Baker, G. A.; Tuckerman, M. E.; Savinell, R. F.; Sangoro, J. R. Deep Eutectic Solvents: A Review of Fundamentals and Applications. *Chem. Rev.* **2021**, *121*, 1232−1285.
(20) Xia, Q. Q.; Chen, C. J.; Yao, Y. G.; Li, J. G.; He, S. M.; Zhou, Y. B.; Li, T.; Pan, X. J.; Yao, Y.; Hu, L. B. A strong, biodegradable and recyclable lignocellulosic bioplastic. *Nat. Sustainable* **2021**, *4*, 627−635.
(21) Wu, J. X.; Liang, Q. H.; Yu, X. L.; Lu, Q. F.; Ma, L. B.; Qin, X. Y.; Chen, G. H.; Li, B. H. Deep eutectic solvents for boosting electrochemical energy storage and conversion: A review and perspective. *Adv. Funct. Mater.* **2021**, *31*, No. 2011102.
(22) Hooshmand, S. E.; Afshari, R.; Ramon, D. J.; Varma, R. S. Deep eutectic solvents: cutting-edge applications in cross-coupling reactions. *Green Chem.* **2020**, *22*, 3668−3692.
(23) Smith, E. L.; Abbott, A. P.; Ryder, K. S. Deep eutectic solvents (DESs) and their applications. *Chem. Rev.* **2014**, *114*, 11060−11082.
(24) Kumar, S.; Sharma, S.; Arumugam, S. M.; Miglani, C.; Elumalai, S. Biphasic separation approach in the DES biomass fractionation facilitates lignin recovery for subsequent valorization to phenolics. *ACS Sustainable Chem. Eng.* **2020**, *8*, 19140−19154.
(25) Mankar, A. R.; Pandey, A.; Modak, A.; Pant, K. J. B. t. Pretreatment of lignocellulosic biomass: A review on recent advances. *Bioresource Technol.* **2021**, *334*, No. 125235.
(26) Gutiérrez, M. C.; Carriazo, D.; Ania, C. O.; Parra, J. B.; Ferrer, M. L.; del Monte, F. Deep eutectic solvents as both precursors and structure directing agents in the synthesis of nitrogen doped hierarchical carbons highly suitable for CO_2 capture. *Energy Environ. Sci.* **2011**, *4*, 3535−3544.
(27) Lu, H.; Zhuang, L. Z.; Gaddam, R. R.; Sun, X. M.; Xiao, C. L.; Duignan, T.; Zhu, Z. H.; Zhao, X. S. Microcrystalline cellulose-derived porous carbons with defective sites for electrochemical applications. *J. Mater. Chem. A* **2019**, *7*, 22579−22587.
(28) Wang, T.; Guo, J.; Guo, Y.; Feng, J.; Wu, D. L. Nitrogen-doped carbon derived from deep eutectic solvent as a high-performance supercapacitor. *ACS Appl. Energy Mater.* **2021**, *4*, 2190−2200.
(29) Xu, Z. X.; Song, H.; Deng, X. Q.; Zhang, Y. Y.; Ma, X. Q.; Tong, S. Q.; He, Z. X.; Wang, Q.; Shao, Y. W.; Hu, X. Dewatering of sewage sludge via thermal hydrolysis with ammonia-treated Fenton iron sludge as skeleton material. *J. Hazard. Mater.* **2019**, *379*, No. 120810.
(30) Fernandez-Lopez, M.; Pedrosa-Castro, G. J.; Valverde, J. L.; Sanchez-Silva, L. Kinetic analysis of manure pyrolysis and combustion processes. *Waste Manage.* **2016**, *58*, 230−240.
(31) Xu, Z. X.; Song, H.; Zhang, S.; Tong, S. Q.; He, Z. X.; Wang, Q.; Li, B.; Hu, X. Co-hydrothermal carbonization of digested sewage sludge and cow dung biogas residue: Investigation of the reaction characteristics. *Energy* **2019**, *187*, No. 115972.
(32) Ge, X.; Gu, C. D.; Wang, X. L.; Tu, J. P. Deep eutectic solvents (DESs)-derived advanced functional materials for energy and environmental applications: challenges, opportunities, and future vision. *J. Mater. Chem. A* **2017**, *5*, 8209−8229.
(33) de Oliveira Silva, J.; Rodrigues, G.; Meireles, C. D.; Ribeiro, S. D.; Vieira, J. G.; da Silva, C. V.; Cerqueira, D. A. Thermal analysis and FTIR studies of sewage sludge produced in treatment plants. The case of sludge in the city of Uberlandia-MG, Brazil. *Thermochim. Acta* **2012**, *528*, 72−75.
(34) Silverstein, R. M.; Webster, F. X.; Kiemle, D. J. *Spectrometric Identification of Organic Compounds*; John wiley & sons, 2014.
(35) de Oliveira, F. C.; Coimbra, J. S. D.; de Oliveira, E. B.; Zuniga, A. D. G.; Rojas, E. E. G. Food protein-polysaccharide conjugates obtained via the Maillard reaction: A review. *Crit. Rev. Food Sci. Nutr.* **2016**, *56*, 1108−1125.
(36) Yin, D. H.; Yin, D. L. The dispersion and solid-state ion exchange of $ZnCl_2$ onto the surface of NaY zeolite using microwave irradiation. *Microporous Mesoporous Mater.* **1998**, *24*, 123−126.
(37) Kuo, C. L.; Wang, C. L.; Ko, H. H.; Hwang, W. S.; Chang, K. M.; Li, W. L.; Huang, H. H.; Chang, Y. H.; Wang, M. C. Synthesis of zinc oxide nanocrystalline powders for cosmetic applications. *Ceram. Int.* **2010**, *36*, 693−698.
(38) García-Martínez, O.; Vila, E.; Vidales, J. L. M. D.; Rojas, R.; Petrov, K. J. J. O. M. S. On the thermal decomposition of the zinc(II) hydroxide chlorides $Zn_5(OH)_8Cl_2{\cdot}H_2O$ and β-Zn(OH)Cl. *J. Mater. Sci.* **1994**, *29*, 5429−5434.
(39) Shan, Y. Q.; Xu, Z. X.; Duan, P. G.; Fan, H. L.; Hu, X.; Luque, R. Nitrogen and sulfur-Doped carbon obtained from direct hydrothermal carbonization of cellulose and ammonium sulfate for supercapacitor applications. *ACS Sustainable Chem. Eng.* **2020**, *8*, 15809−15814.
(40) Paneque, M.; De la Rosa, J. M.; Kern, J.; Reza, M. T.; Knicker, H. Hydrothermal carbonization and pyrolysis of sewage sludges: What happen to carbon and nitrogen? *J. Anal. Appl. Pyrolysis* **2017**, *128*, 314−323.
(41) Chen, H. H.; Rao, Y.; Cao, L. C.; Shi, Y.; Hao, S. L.; Luo, G.; Zhang, S. C. Hydrothermal conversion of sewage sludge: Focusing on the characterization of liquid products and their methane yields. *Chem. Eng. J.* **2019**, *357*, 367−375.
(42) Xu, Z. X.; Xu, L.; Cheng, J. H.; He, Z. X.; Wang, Q.; Hu, X. Investigation of pathways for transformation of N-heterocycle compounds during sewage sludge pyrolysis process. *Fuel Process. Technol.* **2018**, *182*, 37−44.
(43) Mothé, C. G.; de Freitas, J. S. Thermal behavior of cashew gum by simultaneous TG/DTG/DSC-FT-IR and EDXRF. *J. Therm. Anal. Calorim.* **2014**, *116*, 1509−1514.
(44) Peng, C.; Zhai, Y. B.; Zhu, Y.; Xu, B. B.; Wang, T. F.; Li, C. T.; Zeng, G. M. Production of char from sewage sludge employing hydrothermal carbonization: Char properties, combustion behavior and thermal characteristics. *Fuel* **2016**, *176*, 110−118.
(45) Li, Y. H.; Zhang, Y. Q.; Chang, L. P.; Zi, C. Y.; Liang, G. B.; Zhang, D. F.; Xie, W. Analyses on thermal stability of lignites and its derived humic acids. *Energy Sources, Part A* **2020**, *52*, 1−12.
(46) Yao, Z. L.; Ma, X. Q.; Wu, Z. D.; Yao, T. T. TGA-FTIR analysis of co-pyrolysis characteristics of hydrochar and paper sludge. *J. Anal. Appl. Pyrolysis* **2017**, *123*, 40−48.
(47) Xu, Z. X.; Liu, P.; Xu, G. S.; Liu, Q.; He, Z. X.; Wang, Q. Biofuel oil characteristic from catalytic cracking of hydrogenated palm oil. *Energy* **2017**, *133*, 666−675.

https://doi.org/10.1021/acssuschemeng.2c00086
ACS Sustainable Chem. Eng. 2022, 10, 4258−4268